IEEE Photonics Journal
An IEEE Photonics Society Publication

Open Access

Enhanced Far-Field Directional Luminescence Emission by a Hybrid Structure Consisting of Silver Channel and Microlens

Volume 11, Number 3, June 2019

Zhi-Hui Chen
Hongsheng Quan
Yang Wang
Yibiao Yang

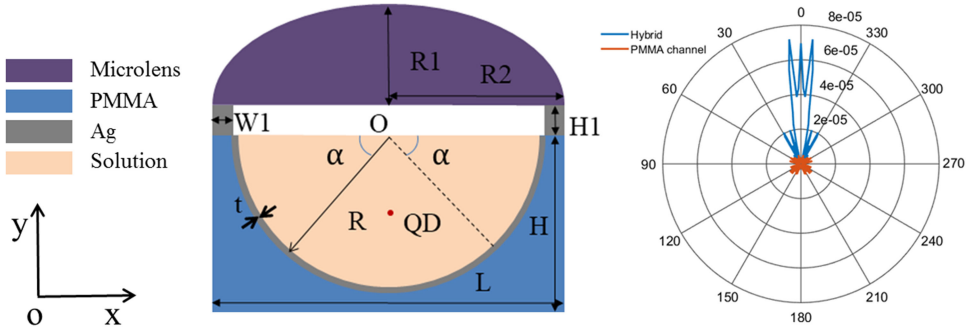

DOI: 10.1109/JPHOT.2019.2918084
1943-0655 © 2019 IEEE

Enhanced Far-Field Directional Luminescence Emission by a Hybrid Structure Consisting of Silver Channel and Microlens

Zhi-Hui Chen,[1] **Hongsheng Quan**,[1] **Yang Wang**,[2] **and Yibiao Yang**[1]

[1]Key Lab of Advanced Transducers and Intelligent Control System, Ministry of Education and Shanxi Province, College of Physics and Optoelectronics, Taiyuan University of Technology, Taiyuan 030024, China
[2]Institute of Biotechnology, Shanxi University, Taiyuan 030006, China

DOI:10.1109/JPHOT.2019.2918084

Manuscript received May 4, 2019; accepted May 14, 2019. Date of publication May 22, 2019; date of current version June 12, 2019. This work was supported in part by the National Natural Science Foundation of China under Grants 11674239, 61575139, 61575138, and 31640019 and in part by Program for the Top Young Talents of Shanxi Province and Sanjin Outstanding Talents, China. This paper has supplementary downloadable material available at http://ieeexplore.ieee.org, provided by the authors. Corresponding author: Zhi-Hui Chen (e-mail: huixu@126.com).

Abstract: In microfluidic detection, the distance between the fluorescent nanoparticles (FNPs) and the structure is usually in far-field range. In previous work, the enhancement of emission will decay exponentially with the increase of the distance between FNPs and the structures, which brings a challenge to the development of high-sensitivity biosensors. In this paper, a hybrid structure consisting of a silver channel and a microlens is proposed to enhance far-field directional emission when the FNP is in far-field range. It is shown that the far-field total power enhancement of our structure is obvious compared to the polymethyl methacrylate channel. This is due to scattering, constructive interference, and resonance modes created by the silver channel and microlens. This structure will contribute to high-sensitivity biosensors.

Index Terms: Directional emission, luminescence, microoptics, microstructure.

1. Introduction

Fluorescent nanoparticles (FNPs) are widely used in light-emitting diodes (LEDs), [1], [2] photocatalytic, [3] biosensors [4]–[7] and bio-imaging. [8] However, the luminescence emission of FNPs is relatively dispersed and the directional emission efficiency is not high, which severely limit their further development in biosensing field. Therefore, it is critical to enhance the directional luminescence emission of FNPs for high sensitivity fluorescence biosensors.

Up to now, some micro/nano structures have been proposed to enhance directional fluorescence/luminescence emission. Metallic planar structures, [9]–[11] antennas, [12]–[15] nanoholes arrays [16] and bull-eye hybrid structures [17]–[19] can induce surface plasmon polaritons (SPPs), which can enhance the excitation and directional emission of FNPs. For example, directional emission was achieved by a split-ring resonator or a single V-shaped nanorod antenna based on the interference between different multipolar moments. [20], [21] But these metal-enhanced emission

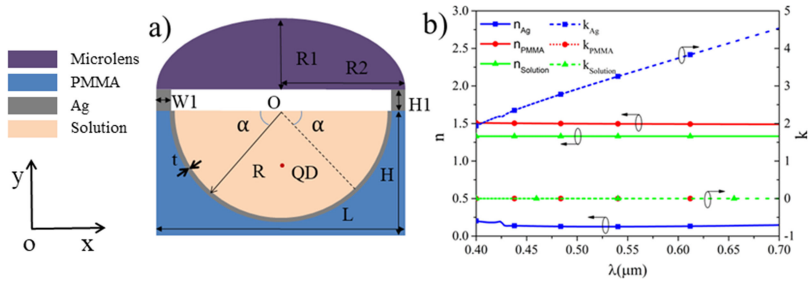

Fig. 1. (a) Schematic of the x-y cross section of the hybrid structure. L = 14 μm, H = 7 μm, R = 6 μm, t = 0.1 μm, W1 = 0.9 μm, H1 = 3 μm, R1 = 1 μm, R2 = 7 μm. (b) The complex refractive indices n and k of silver, PMMA and biological solution in the wavelength range of 400–700 nm. The initial refractive index of the microlens is 1.5.

has certain limitations: (1) the emission will sharply decrease when the distance between FNPs and the metal surface increases, and quenching may happen when the distance is shorter than 10 nm, [22] (2) larger ohmic losses of the metal will reduce the enhancement factor, (3) the large amount of Joule heat generated by ohmic losses will heat up the local environment, which is unsuitable for some temperature-sensitive sensing. [23] In order to solve the above problem, dielectric structures have been proposed to enhance the directional emission of FNPs. [24], [25] The dielectric materials have less absorption loss than metals from visible to near-infrared band, which can reduce the loss of emission. For example, the unique photonic band gap of dielectric photonic crystal (PC) can be utilized to enhance the directional emission of FNPs. [26]–[28] However, the enhancement factor will decay exponentially with the increase of the distance between FNPs and the PC surface. Then, dielectric/metal hybrid structures have been proposed to enhance directional emission of FNPs. [29] However, the distance between the FNPs and the structure is usually in the near-field range.

In microfluidic detection, the distance between the FNPs and the channel is usually in the far-field range, which possesses a challenge to realize high sensitivity fluorescent sensors by using traditional micro/nano structures. Besides, the luminescence of FNP is low and the emission is dispersed, which has a negative effect on the collection of emission signal. Lim *et al.* designed a large dielectric microlens on a large metallic channel that can achieve far-field directional emission. [30] However, its size is relatively large, which is not convenient for the chip integration, and the fluorescence enhancement is not high. Recently, we proposed a sharp convex gold groove [31] and a half-cylindrical gold groove [22] to enhance the directional fluorescence emission in the far-field range, but the enhancement factor is not high due to that the dispersed light can not be well collected, which limits the sensitivity of fluorescence detection.

In this paper, we propose a hybrid structure consisting of a semicircle silver channel and a microlens to enhance directional fluorescence emission. We find that the hybrid structure can achieve far-field directional fluorescence emission enhancement compared to the PMMA channel due to scattering, constructive interference and resonance modes created by the silver channel and microlens. In addition, our structure is experimentally feasible and will contribute to high sensitivity biosensors.

2. Model and Method

The geometrical shapes and sizes of the hybrid structure are shown in Fig. 1(a). We define the center of the silver channel 'O' as the coordinate (0, 0), 'L'/'H' as the width/height of PMMA substrate and 'R' /'t' as the radius/thickness of the silver channel, 'α' as the angle of different silver channel (e.g., it represents a semicircle channel when α is equal to 0, Fig. S1 in supplementary materials), 'H1'/'W1'as the height/width of silver support below the microlens, 'R1'/'R2' as the half short/long axis length of the microlens. Fig. 1(b) shows that the complex refractive indices n and k (n and k represent the real and imaginary parts, respectively) of silver [32], biological solution, and PMMA

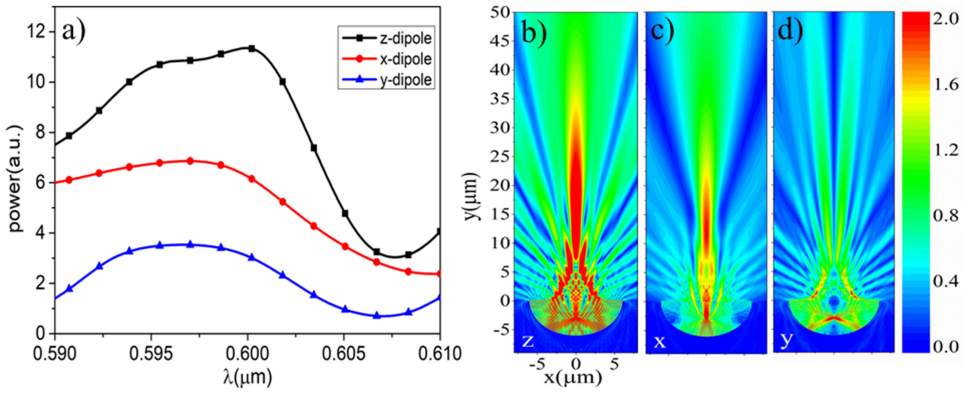

Fig. 2. (a) The far-field total power of the dipole for three different polarizations in the semicircle silver channel, (b-d) the electric field distribution of three different polarizations at wavelength of 600 nm.

[33] varying with the wavelength, respectively. The refractive index of the biological solution is set as 1.33. [34] The initial refractive index of the microlens is 1.5.

In this work, two-dimensional finite difference time domain (FDTD) method [35], [36] is used to investigate the enhanced fluorescence of FNP by the hybrid structure. The simulation area is (x, y) = (−8: 8, −9: 50) μm. The boundary conditions are both perfectly matched layers (PML) in x and y directions. An oscillating electric dipole is used to act as a FNP which is positioned at 3 μm away from the bottom of the silver channel. The central wavelength of FNP is 600 nm, and the full width at half maximum (FWHM) is 20 nm. The explanation of the dipole source is described in supplementary materials. A line power monitor is placed at y = 40 μm to obtain the far-field total directional power of the dipole, in addition, a x-y plane electric field monitor is located at z = 0 μm to calculate the electric field distributions. Far-field pattern is obtained by near-to-far-field transformation analysis, which relies on the field equivalence principle (Huygens' principle) in FDTD method.

3. Results and Discussion

3.1 Directional Emission in Semicircle Silver Channel for Different Polarizations

First, we investigate the effect of semicircle silver channel on fluorescence enhancement at different polarizations. The far-field total power of three polarizations of the dipole is calculated. In Fig. 2(a), the power of dipole oriented in the z-direction is the largest compared to x and y directions. In order to further understand the mechanism, we observe the electric field distribution at wavelength of 600 nm, as shown in Fig. 2(b–d). Compared to x and y polarizations, large-area light reflecting, scattering and interfering occur inside and outside the silver channel in the far-field for z polarization due to the characteristics of the radiation mode. [31], [37] Therefore, we choose z-direction oscillation of dipole in the following study.

3.2 Directional Emission in Silver Channel With Different Angles

Then we investigate the effect of silver channel with different angles on fluorescence directional emission. When α is equal to 0 degree, it is a semicircle, when α is increased/decreased (the angle is positive above the x-axis), the silver channel gradually approaches the perfect circle/arc channel. The far-field total powers for different angles of silver channel are shown in Fig. 3. When α increases from −30 degree to 30 degree, the far-field total power curves oscillate around the power curve of the semicircle. Therefore, we conclude that the effect of channel angle on fluorescence enhancement is negligible. Simultaneously, we find that the power of silver channel at different angle is higher than that of PMMA channel. The maximum power of the semicircle silver channel

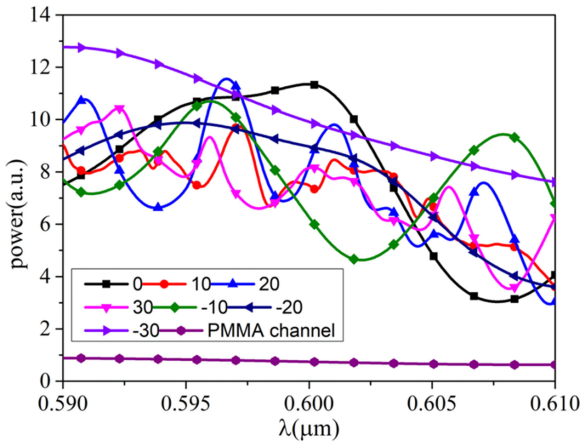

Fig. 3. Far-field total power of silver channel with different angles.

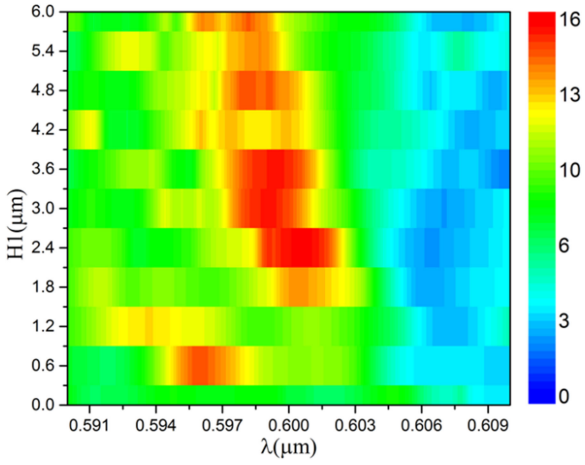

Fig. 4. Far-field total power map of the hybrid structure for different silver support height.

can be up to 15.0 folds compared to PMMA channel. In addition, semicircle silver channel is easier to be fabricated in the experiment, so we choose semicircle silver channel in the following analysis.

3.3 Directional Emission in Hybrid Structure Consisting of Semicircle Silver Channel and Microlens

3.3.1 The Effect of Silver Support on Directional Emission: In order to further enhance the directional emission of fluorescence, we propose a hybrid structure as shown in Fig. 1. Here, we study the effect of silver support on directional emission. The far-field total power is obtained when the height H1 of the support varies from 0 to 6 μm as shown in Fig. 4. When H1 is in the range of 2 $\sim$ 4 μm, the hybrid structure can achieve high directional emission at the center wavelength 0.6 μm. This is because that the Ag support changes the optical path from semicircle silver channel to microlens, thus allowing the light to undergo sufficient phase changes before the light reaches the microlens, and finally achieve better interference in the far field than the situation without Ag support. [30] Here we choose H1 $=$ 3 μm in the following calculations.

3.3.2 The Effect of the Height and Refractive Index of the Microlens on Directional Emission: We obtain the far-field total power when the height of the microlens varies from 1 μm to 6 μm as

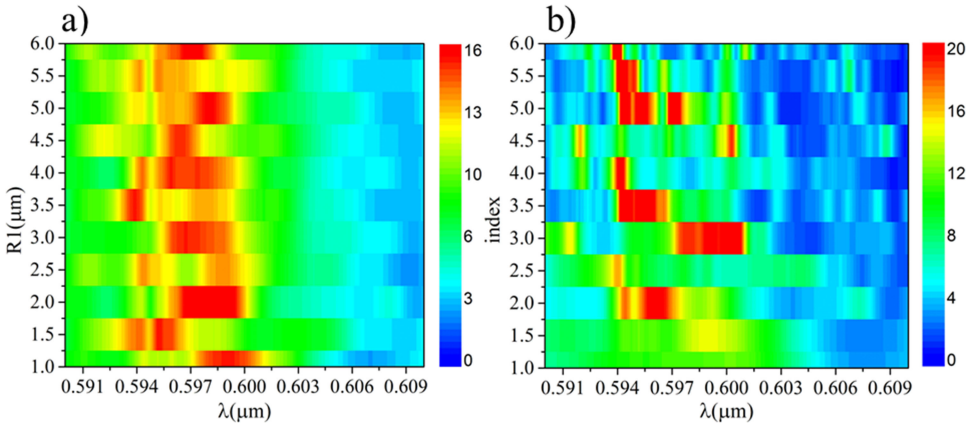

Fig. 5. Far-field total power map of the hybrid structure with (a) different height of the microlens, (b) different refractive index of the microlens.

shown in Fig. 5(a). We find that the height of the microlens has little effect on the fluorescence enhancement in the long wavelength, while it has a significant effect in the short band. When the height of the microlens is 1 μm, large directional fluorescence power can be achieved at around the central wavelength of FNP, therefore, we choose R1 $=$ 1 μm in the following study. Then, we study the effect of the refractive index of the microlens on directional emission, the far-field total power shown in Fig. 5(b) is obtained when the refractive index of the microlens varies from 1 to 6. When the refractive index of the microlens changes, there is little effect on the fluorescence enhancement in the long wavelength band, while the enhancement is different in the short wavelength band. In particular, when the refractive index of the microlens is 3.0, large fluorescence enhancement can be achieved around the central wavelength of FNP. Therefore, we study the directional emission enhancement of the hybrid structure when the refractive index of the microlens is 3.0 in the following study.

Based on the above research, we get the optimized parameters of the hybrid structure: L $=$ 14 μm, H $=$ 7 μm, R $=$ 6 μm, t1 $=$ 0.1 μm, H1 $=$ 3 μm, W1 $=$ 0.9 μm, R1 $=$ 1 μm, R2 $=$ 7 μm, $n_{microlens}$ $=$ 3. Then we analyze the far-field total power and far-field angular radiation distribution of the FNP in optimized hybrid structure, semicircle silver channel and the PMMA channel, respectively, as shown in Fig. 6. In Fig. 6(a), the far-field total power of the optimized hybrid structure is the largest compared to the other structures. The far-field radiation patterns [38], [39] corresponding to the center wavelength of FNP in the optimized hybrid structure and PMMA channel are shown in Fig. 6(b). The spatial electric field distribution |E| for the cases of PMMA channel and the optimized hybrid structure are shown in Fig. 6(c–d), respectively. The optimized hybrid structure can achieve stronger far-field total power and more converging emission compared to the PMMA channel. Besides, the highly directional emission can also be achieved in the 3D simulation, which confirm the validity of the 2D simulation results (Fig. S2 in the supplementary materials).

We select 11 typical positions as shown in Fig. 7(a) for analysis. We obtain the sum of the far-field total power of the hybrid structure, semicircle silver channel and PMMA channel for these positions, as shown in Fig. 7(b). The hybrid structure can achieve maximum far-field total power compared to semicircle silver channel and PMMA channel, which proves the outstanding performance of our structure in enhancing directional luminescence emission. The sum of far-field radiation patterns corresponding to the central wavelength of FNP at all the positions in the optimized hybrid structure are shown in Fig. 7(c), the emission is of good directionality. Besides, we proves that our optimized structure can achieve good directional emission by using 17 different dipole's positions (Fig. S3 in supplementary materials). Our system is complicated, for example, the particle position is random, and the representative position is selected in the calculation, so the result will have some reasonable error due to the approximations.

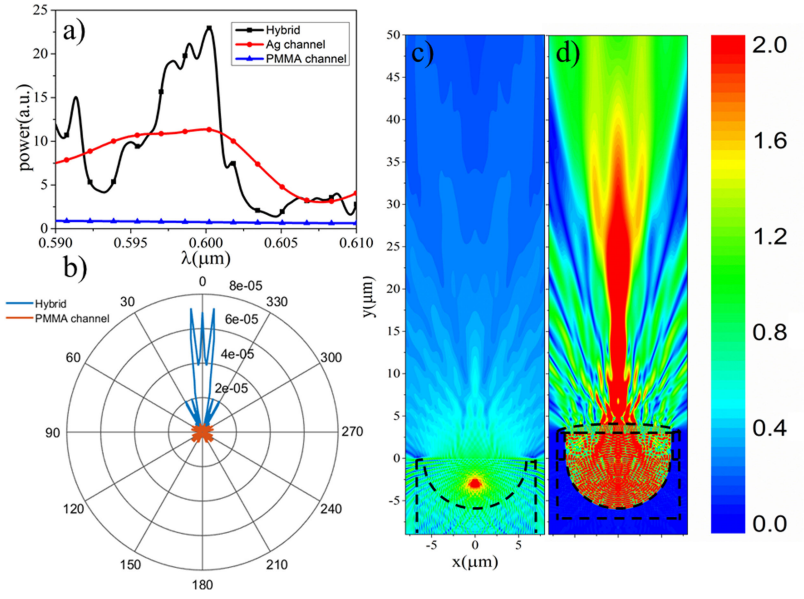

Fig. 6. (a) Far-field total power of optimized hybrid structure, semicircle silver channel and PMMA channel, (b) Far-field angular radiation patterns of optimized hybrid structure and PMMA channel, (c–d) Electric field distribution of the PMMA channel and optimized hybrid structure at wavelength of 600 nm.

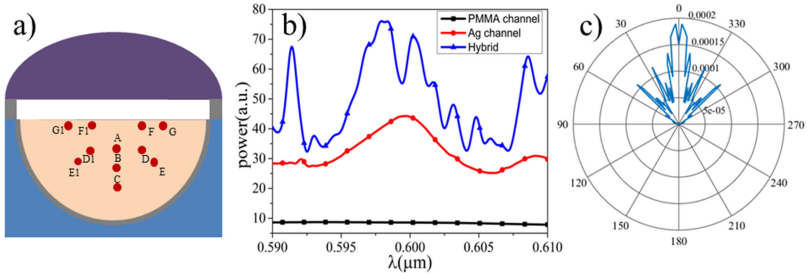

Fig. 7. (a) Schematic of the hybrid structure and 11 typical positions of FNPs, such as A(0, −2) μm, B(0,−3) μm, C(0, −4) μm, D(2.121, −2.121) μm, D1(−2.121, −2.121) μm, E(2.828, −2.828) μm, E1(−2.828, −2.828) μm, F(2, −0.5) μm, F1(−2, −0.5) μm, G(3, −0.5) μm, G1(−3, −0.5) μm (b) The sum of far-field power for different positions of FNPs, (c) The sum of far-field angular radiation patterns of all the positions.

4. Conclusion

In conclusion, a hybrid structure consisting of a semicircle silver channel and a microlens is proposed to enhance directional fluorescence emission. We systematically study the far-field total power and the far-field radiation pattern. We find that the hybrid structure can achieve far-field directional fluorescence emission enhancement due to scattering, constructive interference and resonance modes. The total power enhancement of our structure is obvious compared to PMMA channel. If the enhancement of excitation is also included, the emission is anticipated to be further enhanced. This work will greatly contribute to the development of high sensitivity fluorescence biosensors.

Acknowledgment

Conflicts of interest: There are no conflicts of interest to declare.

References

[1] X. Dai *et al.*, "Solution-processed, high-performance light-emitting diodes based on quantum dots," *Nature*, vol. 515, pp. 96–99, 2014.
[2] Z. Zhang *et al.*, "High-performance, solution-processed, and insulating-layer-free light-emitting diodes based on colloidal quantum dots," *Adv. Mater.*, vol. 30, 2018, Art. no. 1801387.
[3] J. Wang *et al.*, "Facile gel-based morphological control of Ag/g-C3N4 porous nanofibers for photocatalytic hydrogen generation," *ACS Sustain. Chem. Eng.*, vol. 5, pp. 10633–10639, 2017.
[4] C. M. Courtney, S. M. Goodman, J. A. McDaniel, N. E. Madinger, A. Chatterjee, and P. Nagpal, "Photoexcited quantum dots for killing multidrug-resistant bacteria," *Nature Mater.*, vol. 15, pp. 529–534, 2016.
[5] B. Dubertret, "DNA detectives," *Nature Mater.*, vol. 4, pp. 797–798, 2005.
[6] K. J. McHugh *et al.*, "Biocompatible semiconductor quantum dots as cancer imaging agents," *Adv. Mater.*, vol. 30, 2018, Art. no. 1706356.
[7] H. Xu *et al.*, "Metal–organic framework nanosheets for fast-response and highly sensitive luminescent sensing of Fe3+," *J. Mater. Chem. A*, vol. 4, pp. 10900–10905, 2016.
[8] Y. Ma *et al.*, "Live cell imaging of single genomic loci with quantum dot-labeled TALEs," *Nature Commun.* vol. 8, 2017, Art. no. 15318.
[9] N. Calander, "Surface plasmon-coupled emission and fabry−perot resonance in the sample layer: A theoretical approach," *J. Phys. Chem. B*, vol. 109, pp. 13957–13963, 2005.
[10] S. Dutta Choudhury, R. Badugu, and J. R. Lakowicz, "Directing fluorescence with plasmonic and photonic structures," *Accounts Chem. Res.*, vol. 48, pp. 2171–2180, 2015.
[11] J. R. Lakowicz, "Radiative decay engineering 3. Surface plasmon-coupled directional emission," *Analytical Biochem.*, vol. 324, pp. 153–169, 2004.
[12] N. Dorh *et al.*, "Nanoantenna arrays combining enhancement and beam control for fluorescence-based sensing applications," *Appl. Opt.*, vol. 56, pp. 8252–8256, 2017.
[13] X. Meng, R. R. Grote, J. I. Dadap, N. C. Panoiu, and R. M. Osgood, "Engineering metal-nanoantennae/dye complexes for maximum fluorescence enhancement," *Opt. Exp.*, vol. 22, pp. 22018–22030, 2014.
[14] G. Vecchi, V. Giannini, and J. Gómez Rivas, "Shaping the fluorescent emission by lattice resonances in plasmonic crystals of nanoantennas," *Phys. Rev. Lett.*, vol. 102, 2009, Art. no. 146807.
[15] Z. Chen, L. He, Y. Wang, and Z. Gan, "Effects of size and distribution of silver nanoparticles on directional fluorescence emission enhancement," *IEEE Photon. J.*, vol. 9, no. 1, Feb. 2017, Art. no. 4500108.
[16] Y. Wang *et al.*, "Directional fluorescence emission co-enhanced by localized and propagating surface plasmons for biosensing," *Nanoscale*, vol. 8, pp. 8008–8016, 2016.
[17] S. K. H. Andersen *et al.*, "Hybrid plasmonic bullseye antennas for efficient photon collection," *ACS Photon.*, vol. 5, pp. 692–698, 2018.
[18] H. Aouani *et al.*, "Bright unidirectional fluorescence emission of molecules in a nanoaperture with plasmonic corrugations," *Nano Lett.*, vol. 11, pp. 637–644, 2011.
[19] H. Aouani, O. Mahboub, E. Devaux, H. Rigneault, T. W. Ebbesen, and J. Wenger, "Plasmonic antennas for directional sorting of fluorescence emission," *Nano Lett.*, vol. 11, pp. 2400–2406, 2011.
[20] I. M. Hancu, A. G. Curto, M. Castro-López, M. Kuttge, and N. F. van Hulst, "Multipolar interference for directed light emission," *Nano Lett.*, vol. 14, pp. 166–171, 2014.
[21] D. Vercruysse *et al.*, "Directional fluorescence emission by individual V-antennas explained by mode expansion," *ACS Nano*, vol. 8, pp. 8232–8241, 2014.
[22] Z.-H. Chen, L. Liang, Y. Wang, and Y. Yang, "Spatial remote luminescence enhancement by a half-cylindrical Au groove," *J. Mater. Chem. C*, vol. 4, pp. 11321–11327, 2016.
[23] R. Regmi *et al.*, "All-dielectric silicon nanogap antennas to enhance the fluorescence of single molecules," *Nano Lett.*, vol. 16, pp. 5143–5151, 2016.
[24] N. Qiao, Z. Chen, Y. Yang, S. Liu, Y. Wang, and H. Ye, "Enhancing the brightness of quantum dot light-emitting diodes by multilayer heterostructures," *IEEE Photon. J.*, vol. 8, no. 2, Apr. 2016, Art. no. 1600407.
[25] Z.-H. Chen *et al.*, "Tunable high reflective bands to improve quantum dot white light-emitting diodes," *J. Mater. Chem. C*, vol. 5, pp. 1149–1154, 2017.
[26] Z.-H. Chen, Y. Wang, Y. Yang, N. Qiao, Y. Wang, and Z. Yu, "Enhanced normal-direction excitation and emission of dual-emitting quantum dots on a cascaded photonic crystal surface," *Nanoscale*, vol. 6, pp. 14708–14715, 2014.
[27] E. Eftekhari *et al.*, "Anomalous fluorescence enhancement from double heterostructure 3D colloidal photonic crystals–a multifunctional fluorescence-based sensor platform," *Sci. Rep.*, vol. 5, 2015, Art. no. 14439.
[28] F. Frascella *et al.*, "Enhanced fluorescence detection of miRNA-16 on a photonic crystal," *Analyst*, vol. 140, pp. 5459–5463, 2015.
[29] A. Devilez, B. Stout, and N. Bonod, "Compact metallo-dielectric optical antenna for ultra directional and enhanced radiative emission," *ACS Nano*, vol. 4, pp. 3390–3396, 2010.
[30] J. Lim, P. Gruner, M. Konrad, and J.-C. Baret, "Micro-optical lens array for fluorescence detection in droplet-based microfluidics," *Lab Chip*, vol. 13, pp. 1472–1475, 2013.
[31] Z.-H. Chen, H. Shi, Y. Wang, Y. Yang, S. Liu, and H. Ye, "Sharp convex gold grooves for fluorescence enhancement in micro/nano fluidic biosensing," *J. Mater. Chem. B*, vol. 5, pp. 8839–8844, 2017.
[32] E. D. Palik, "Preface," *in Handbook of Optical Constants of Solids*, E. D. Palik, Ed. New York, NY, USA: Academic, 1997, pp. 17–18.
[33] G. Beadie, M. Brindza, R. A. Flynn, A. Rosenberg, and J. S. Shirk, "Refractive index measurements of poly(methyl methacrylate) (PMMA) from from 0.4-1.6 μm," *Appl. Opt.*, vol. 54, pp. F139–F143, 2015.

[34] C. L. Tregidgo, J. A. Levitt, and K. Suhling, "Effect of refractive index on the fluorescence lifetime of green fluorescent protein," *Proc. SPIE*, vol. 13, 2008, Art. no. 031218.
[35] Y. Kane, "Numerical solution of initial boundary value problems involving maxwell's equations in isotropic media," *IEEE Trans. Antennas Propag.*, vol. 14, no. 3, pp. 302–307, May 1966.
[36] A. Taflove, S. C. Hagness, and M. Piket-May, "9 - computational electromagnetics: The finite-difference time-domain method," in *The Electrical Engineering Handbook*, W.-K. Chen, Ed. New York, NY, USA: Academic, 2005, pp. 629–670.
[37] M. Bauch, K. Toma, M. Toma, Q. Zhang, and J. Dostalek, "Plasmon-enhanced fluorescence biosensors: A review," *Plasmonics*, vol. 9, pp. 781–799, 2014.
[38] J. Yang, J.-P. Hugonin, and P. Lalanne, "Near-to-far field transformations for radiative and guided waves," *ACS Photon.*, vol. 3, pp. 395–402, 2016.
[39] P. Zhang, P. Ren, and X.-W. Chen, "On the emission pattern of nanoscopic emitters in planar anisotropic matrix and nanoantenna structures," *Nanoscale*, 2019, doi: 10.1039/C9NR00235A.